Isospin dependence of Pauli corrections to the pion-nucleus optical potential

H.-C. Chiang* and Mikkel B. Johnson
Los Alamos National Laboratory, Los Alamos, New Mexico 87545
(Received 16 April 1985)

We examine how the Pauli exclusion principle affects the pion-nucleus optical potential U in the region of the Δ_{33} resonance, i.e., for pion kinetic energies of 50—300 MeV. In our formulation the exchange effects enter through n-body correlation functions and contribute to U as higher-order corrections in a density expansion. We study the rate of convergence of the expansion and derive an integral equation that sums selected exchange terms to all orders. We calculate the isoscalar, isovector, and isotensor components of U for the cases of infinite nuclear matter and finite nuclei. We identify the limiting conditions under which our treatment of the Pauli effect reduces to that in more familiar approaches.

I. INTRODUCTION

The availability of pion charge exchange data in recent years has led to a renewed interest in understanding dynamical modifications to the pion-nucleus and Δ_{33}-nucleus interaction, especially the isospin-dependent pieces of these interactions. A recent phenomenological analysis[1] of pion elastic, single-, and double-charge-exchange data has provided a quantitative characterization of the second-order medium corrections that are required by the data when the pion optical potential U is expressed in the form

$$\hat{\mathbf{U}} = U_0 + U_1(\boldsymbol{\phi}\cdot\mathbf{T}) + U_2(\boldsymbol{\phi}\cdot\mathbf{T})^2 , \tag{1}$$

where $\boldsymbol{\phi}$ is the pion and $\mathbf{T}$ the nucleus isotopic spin operator and where U_0, U_1, and U_2 are referred to as the isoscalar, isovector, and isotensor components of the optical potential. The origin of the large second-order corrections found in Ref. 1 is not established theoretically, and the purpose of this paper is to study in detail one such correction, i.e., arising from the Pauli exclusion principle.

There have been studies of the Pauli exclusion principle for pion scattering in many contexts.[2–14] The investigation in the current paper relies on a method that we feel to be particularly well suited to the optical potential formulation. In particular, we use the diagrammatic expansion for U of Ref. 15, in which the Pauli exclusion principle enters through well-defined multibody correlation functions. The contribution to U_0, U_1, and U_2 arising from the leading term in this expansion was evaluated in Ref. 14. Because this term was found to be large, one might expect higher-order terms in the expansion to be important. The main aim of the current paper is to examine the rate of convergence of the representation of the Pauli effect in the formalism of Ref. 15.

In Sec. II we enumerate the types of exchange terms that occur in the expansion in Ref. 15 and select an important subset of them. In Sec. III we derive an integral equation that sums these terms, and describe a method for determining U_0, U_1, and U_2 from the solution. Section IV specializes to the case of infinite nuclear matter and Sec. V introduces a surface correction that permits an approximate treatment for finite nuclei.

In Secs. VI and VII we compare our results to other approaches. Section VI introduces the eikonal approximation, which makes possible the assessment of how well the Pauli principle is represented in the Glauber theory treatment of pion scattering. Section VII shows the connection between our representation of Pauli effects through correlation functions and the more common procedure of expanding U in terms of an effective pion-nucleon scattering amplitude that excludes intermediate states that are normally occupied in the nuclear ground state. In Sec. VIII we present numerical results, and in Sec. IX we summarize our results and present our conclusions.

II. THE DENSITY EXPANSION

In Ref. 15, a diagrammatic expansion for the pion optical potential U is described. The antisymmetry of the wave function influences U through exchange terms that occur as n-body correlation functions. In this section we want to focus on a subset of these exchange terms and sum them to all orders. In this fashion we are able to study the convergence of the Pauli correction to the multiple scattering expansion of U.

In the theory of Ref. 15, the optical potential is the proper self-energy of the pion Green's function. The free Green's function propagates pions forward in time as particles and backward as antiparticles. Examples of terms that occur in this expansion are shown in Fig. 1. Figure 1(a) shows the exchange term corresponding to Fig. 1(b), which is the sequential scattering of a pion from two nucleons. The diagrams are similar to Feynman diagrams and the rules for evaluating them are given in Ref. 15. Because we are interested here in the Pauli effect, we quote only one rule, which is that each diagram should be given an overall sign $(-)^{l+h}$ where h is the number of explicit nucleon "hole" lines (corresponding to orbitals in the normally occupied ground state) and l is the number of closed loops. In Fig. 1(a), $l+h=3$ and in Fig. 1(b), $l+h=2$, therefore there is a relative minus sign, which may be traced directly to the antisymmetry of the wave

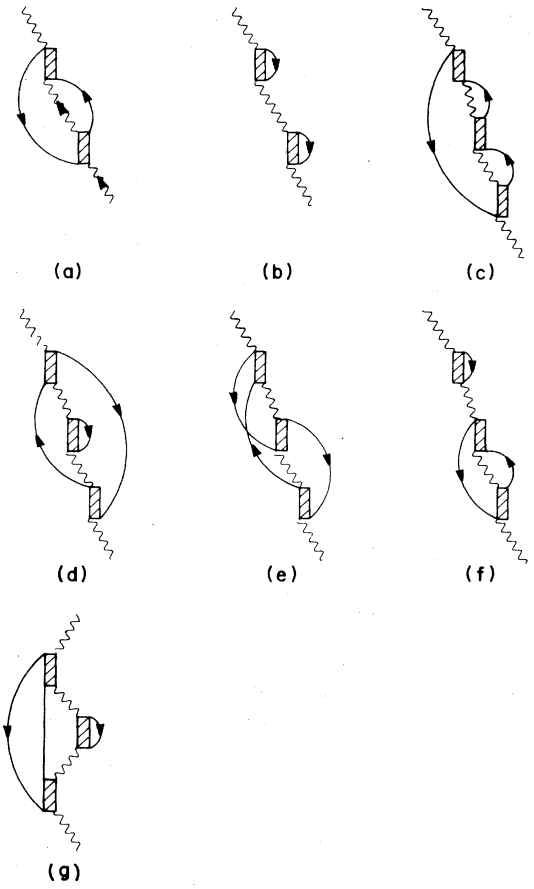

FIG. 1. Examples of diagrams contribute to pion-nucleus elastic scattering.

function. The shaded boxes represent the pion-nucleon scattering amplitude. We want to now consider the exchange terms corresponding to the sequential scattering of the pion from an arbitrary number of nucleons through the pion-nucleon scattering amplitude. There are three such terms in third order, and they are shown in Fig. 1(c)—(e). The reducible terms such as those shown in Fig. 1(b) and (f) will not be considered further here.

We now want to classify the diagrams as follows. The term in Fig. 1(d) is clearly a medium modification of the intermediate pion propagator. In our calculations we shall always allow pions in intermediate states to propagate as dressed pions, and to streamline the notation we will never draw diagrams in which pions have explicit self-energy insertions. Among the diagrams involving exchange of nucleon lines are thus left with the simple sequential term in Fig. 1(c) and the more complicated "intertwined" contribution of Fig. 1(e). The intertwined diagrams in which some intermediate nucleon lines are crossed will not be considered further in this paper. These are topologically similar to exchanges of more complicated irreducible terms and should be considered separately along with their direct counterpart. For example, Fig. 1(e) and the multiple reflection in Fig. 1(g) are similar and should be considered together at a later time.

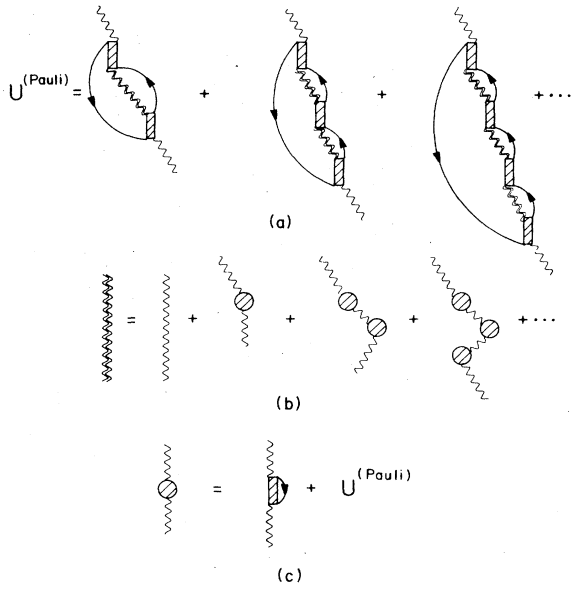

FIG. 2. Diagrammatic definition of $U^{(\mathrm{Pauli})}$.

The Pauli corrections to sequential scattering are therefore the series drawn in Fig. 2(a). We will show the effect of summing all terms of this form in order to study the convergence of the theory. In Sec. VII we demonstrate that the sum of these terms gives, in a well-defined limit, the more familiar G-matrix prescription for including the Pauli effect, namely excluding the intermediate states of the free pion nucleon amplitide that lie below the Fermi surface. The pion propagators in Fig. 2(a) are, as stated, modified by the pion interactions with the nuclear medium, as shown in Fig. 2(b). We include, as a first approximation, all dressings of the pion which can be described by the lowest order optical potential, the first term on the right-hand side of Fig. 2(c). The effect of including our $U^{(\mathrm{Pauli})}$ correction, the second term on the right-hand side of Fig. 2(c), is also shown.

III. SCATTERING THEORY

In this work, we ignore the spin-dependent part of pion-nucleon amplitude and assume that the P wave dominates the πN scattering amplitude. For the purposes of this work we evaluate the Pauli corrections for fixed nucleon sources.[15(a)] For the πN scattering amplitude corresponding to nucleon i, we then take

$$\hat{\mathbf{F}}_i(\mathbf{k}',\mathbf{k})=\left[\frac{k_0^2}{3}\right]\hat{\boldsymbol{\lambda}}_i\frac{v(k')v(k)}{v^2(k_0)}\sum_m Y_{1m}(\hat{\mathbf{k}}')Y_{1m}^*(\hat{\mathbf{k}})\ . \tag{2}$$

The contribution to the pion-nucleus optical potential arising from the spin dependent part in the pion-nucleon amplitude is small; to include this part is trivial but tedious, and we ignore it here. The isospin dependence is included in the operator

$$\hat{\boldsymbol{\lambda}}_i=\lambda_{00}+\tfrac{1}{2}\lambda_{01}\boldsymbol{\phi}\cdot\boldsymbol{\tau}_i\ , \tag{3}$$

where λ_{00} and λ_{01} characterize the scalar-isoscalar and

scalar-isovector πN scattering amplitudes and where $\boldsymbol{\phi}$ is the pion isospin operator and $\boldsymbol{\tau}_i$ is the isospin operator for a nucleon. $v(k)$ is the form factor for pion-nucleon coupling.

We define a set of isospin states for the pion-nucleon system.

$$V(\pi^+\mathrm{p})=\begin{bmatrix}1\\0\\0\\0\\0\\0\end{bmatrix}\equiv V_1\ ;\quad V(\pi^+\mathrm{n})=\begin{bmatrix}0\\1\\0\\0\\0\\0\end{bmatrix}\equiv V_2\ ;$$

$$V(\pi^0\mathrm{p})=\begin{bmatrix}0\\0\\1\\0\\0\\0\end{bmatrix}\equiv V_3\ ;\quad V(\pi^0\mathrm{n})=\begin{bmatrix}0\\0\\0\\1\\0\\0\end{bmatrix}\equiv V_4\ ; \tag{4}$$

$$V(\pi^-\mathrm{p})=\begin{bmatrix}0\\0\\0\\0\\1\\0\end{bmatrix}\equiv V_5\ ;\quad V(\pi^-\mathrm{n})=\begin{bmatrix}0\\0\\0\\0\\0\\1\end{bmatrix}\equiv V_6\ ,$$

and the matrix

$$\tilde{F}=\begin{bmatrix}f_{11}&0&0&0&0&0\\0&f_{22}&f_{23}&0&0&0\\0&f_{32}&f_{33}&0&0&0\\0&0&0&f_{44}&f_{45}&0\\0&0&0&f_{54}&f_{55}&0\\0&0&0&0&0&f_{66}\end{bmatrix}, \tag{5}$$

where

$$f_{11}=f_{66}=-4\pi(k_0^2/3)(\lambda_{00}+\tfrac{1}{2}\lambda_{01})\ ; \tag{6}$$

$$f_{22}=f_{55}=-4\pi(k_0^2/3)(\lambda_{00}-\tfrac{1}{2}\lambda_{01})\ ; \tag{7}$$

$$f_{33}=f_{44}=-4\pi(k_0^2/3)\lambda_{00}\ ; \tag{8}$$

$$f_{23}=f_{32}=f_{45}=f_{54}=-2\sqrt{2}\pi(k_0^2/3)\lambda_{01}\ . \tag{9}$$

The rest of the elements of $\tilde{F}$ are zero. For a given m the physical πN scattering amplitudes can be related to $\tilde{F}$ by the following expressions:

$$f_{\pi^+\mathrm{p}\to\pi^+\mathrm{p}}=f_{\pi^-\mathrm{n}\to\pi^-\mathrm{n}}=\langle V_1\mid\tilde{F}\mid V_1\rangle\left[\frac{-1}{4\pi}\right]\sum_m Y_{1m}(\hat{\mathbf{k}}')Y_{1m}^*(\hat{\mathbf{k}})\ , \tag{10}$$

$$f_{\pi^+\mathrm{n}\to\pi^0\mathrm{p}}=f_{\pi^-\mathrm{p}\to\pi^0\mathrm{n}}=\langle V_2\mid\tilde{F}\mid V_1\rangle\left[\frac{-1}{4\pi}\right]\sum_m Y_{1m}(\hat{\mathbf{k}}')Y_{1m}^*(\hat{\mathbf{k}})\ . \tag{11}$$

We divide the diagrams into two classes: (1) the incoming pion interacts first with a proton in the nucleus; (2) the incident pion starts the interaction with a neutron in the nucleus. The total contribution to the optical potential is the sum of these two. Therefore, we can define the optical potential as a 6×6 matrix, $\tilde{U}$. The diagonal elements of $\tilde{U}$, namely U_{11}, U_{33}, and U_{55}, correspond to the optical potentials for which π^+, π^0, and π^- interact first with a proton in the nucleus, respectively; and U_{22}, U_{44}, and U_{66} are the optical potentials for which π^+, π^0, and π^- scatter first with a neutron in the nucleus during a multiple scattering process. Then π^+-, π^0-, and π^--nucleus optical potentials can be written as follows:

$$U^{(+)}=\langle V_1\mid\tilde{U}\mid V_1\rangle+\langle V_2\mid\tilde{U}\mid V_2\rangle\ ; \tag{12}$$

$$U^{(0)}=\langle V_3\mid\tilde{U}\mid V_3\rangle+\langle V_4\mid\tilde{U}\mid V_4\rangle\ ; \tag{13}$$

$$U^{(-)}=\langle V_5\mid\tilde{U}\mid V_5\rangle+\langle V_6\mid\tilde{U}\mid V_6\rangle\ . \tag{14}$$

To evaluate Figs. 2(a)–(c) we define the operators $T^{(2)}$, $T^{(3)}$, $T^{(4)}$, . . . , to be 6×6 matrices. According to the rules specified in Ref. 15, we have

$$T_{jj'}^{(2)}(\mathbf{k}',\mathbf{k};\mathbf{r}_f-\mathbf{r}_i)=\frac{v(k')v(k)}{v^2(k_0)}\sum_m Y_{1m}(\hat{\mathbf{k}}')Y_{1m}^*(\hat{\mathbf{k}})\left[\sum_{j''}\tilde{F}_{jj''}I_{j''j'}^{(m)}(\mathbf{r}_f-\mathbf{r}_i)\right], \tag{15a}$$

$$T_{jj'}^{(3)}(\mathbf{k}',\mathbf{k};\mathbf{r}_f-\mathbf{r}_A,\mathbf{r}_A-\mathbf{r}_i)=-\frac{v(k')v(k)}{v^2(k_0)}\sum_m Y_{1m}(\hat{\mathbf{k}}')\left[\sum_{j'',j'''}\tilde{F}_{jj''}I_{j''j'''}^{(m)}(\mathbf{r}_f-\mathbf{r}_A)I_{j'''j'}^{(m)}(\mathbf{r}_A-\mathbf{r}_i)\right]Y_{1m}^*(\hat{\mathbf{k}})\ , \tag{16a}$$

$$T_{jj'}^{(4)}(\mathbf{k}',\mathbf{k};\mathbf{r}_f-\mathbf{r}_A,\mathbf{r}_A-\mathbf{r}_B,\mathbf{r}_B-\mathbf{r}_i)=\frac{v(k')v(k)}{v^2(k_0)}\sum_m Y_{1m}(\hat{\mathbf{k}}')\left[\sum_{j'',j''',j''''}\tilde{F}_{jj''}I_{j''j'''}^{(m)}(\mathbf{r}_f-\mathbf{r}_A)\times I_{j'''j''''}^{(m)}(\mathbf{r}_A-\mathbf{r}_B)I_{j'''',j'}^{(m)}(\mathbf{r}_B-\mathbf{r}_i)\right]Y_{1m}^*(\hat{\mathbf{k}})\ , \tag{17a}$$

or

$$T_{jj'}^{(2)}(\mathbf{k}',\mathbf{k};\mathbf{r}_A-\mathbf{r}_B)=\frac{v(k')v(k)}{v^2(k_0)}\sum_m Y_{1m}(\hat{\mathbf{k}}')Y_{1m}^*(\hat{\mathbf{k}})\left[\sum_{j''}\tilde{F}_{jj''}I_{j''j'}^{(m)}(\mathbf{r}_A-\mathbf{r}_B)\right]. \tag{15b}$$

$$T^{(3)}_{jj'}(\mathbf{k}',\mathbf{k};\mathbf{r}_A-r_B,\mathbf{r}_B-\mathbf{r}_C)=-\sum_{j''}T^{(2)}_{jj''}I^{(m)}_{j''j'}(\mathbf{r}_B-\mathbf{r}_C)\ , \tag{16b}$$

$$T^{(4)}_{jj'}(\mathbf{k}',\mathbf{k};\mathbf{r}_A-\mathbf{r}_B,\mathbf{r}_B-\mathbf{r}_C,\mathbf{r}_C-\mathbf{r}_D)=-\sum_{j''}T^{(3)}_{jj''}I^{(m)}_{j''j'}(\mathbf{r}_C-\mathbf{r}_D)\ . \tag{17b}$$

The generalization to more than four struck nucleons is obvious. Here $I^{(m)}$ is a 6×6 matrix,

$$I^{(m)}_{jj'}(\mathbf{r})=\tilde{F}_{jj'}\int\frac{d^3k_1}{(2\pi)^3}\frac{v^2(k_1)}{v^2(k_0)}Y^*_{1m}(\hat{\mathbf{k}}_1)$$

$$\times\Gamma(r)g(\mathbf{k}_1,\mathbf{r})Y_{1m'}(\hat{\mathbf{k}}_1)\,|_{\,m=m'}\ . \tag{18}$$

It is sufficient to consider only the diagonal matrix elements in the magnetic quantum number m for reasons explained below. In Eq. (18) $\mathbf{k}$ and $\mathbf{k}'$ are the incident and outgoing momenta of the pion, respectively, $\mathbf{r}$ is the relative coordinate of successively struck nucleons, and g is a pion propagator in the nucleus,

$$g(\mathbf{k},\mathbf{r})=\frac{e^{+i\mathbf{k}\cdot\mathbf{r}}}{k_0^2-k^2+W+i\eta}\ . \tag{19}$$

Here $\Gamma(r)$ is the pair distribution function of the two nucleons and W is a complex number that characterizes the mean free path of the pion in the nucleus. W is related to the first-order pion-nucleus optical potential,

$$W(R,E)=-k_0^2\rho(R)\lambda_{00}\left[1+\frac{\nabla^2\rho(r)}{2k_0^2\rho(R)}\right]\ . \tag{20}$$

Finally, the pion-nucleus optical potential from Pauli exchange multiple scattering can be written,

$$\tilde{U}^{(\mathrm{Pauli})}(\mathbf{k}',\mathbf{k})=\sum_\gamma\left[\sum_{\substack{\text{all}\\ \text{occupied}\\ \text{states}}}\langle\langle e^{-i\mathbf{k}'\cdot\mathbf{r}_f}T^{(\gamma)}e^{i\mathbf{k}\cdot\mathbf{r}_i}\rangle\rangle\right]\ , \tag{21}$$

where the double angular brackets mean that we average over nuclear wave functions, keeping only the sequence in Fig. 2.

Following Ref. 15, we calculate elastic scatterings, and then by applying isotopic spin invariance the isoscalar, isovector, and isotensor parts of the optical potential can be generated,[14] namely,

$$U_2=(U^{(+)}+U^{(-)}-2U^{(0)})/[T(2T-1)]\ , \tag{22}$$

$$U_1=(U^{(0)}-U^{(+)})/T+TU_2\ , \tag{23}$$

$$U_0=U^{(0)}-TU_2\ . \tag{24}$$

IV. THE OPTICAL POTENTIAL FOR INFINITE NUCLEAR MATTER

As discussed in Ref. 14 the sum over all occupied states of a hole line extending between two nucleons leads to

$$\sum_A\rightarrow\frac{\rho_j(0)}{2}S(k_{Fj}r) \tag{25}$$

where we define

$$\mathbf{r}=\mathbf{r}_A-\mathbf{r}_B \tag{26}$$

and where $\rho_j(0)$ is the density of nuclear matter of particles of type j (j=neutrons, protons) and $S(k_Fr)$ is the Slater function,

$$S(k_{Fj}r)=\frac{2}{\rho_j(0)}\int\frac{d^3k}{(2\pi)^3}e^{i\mathbf{k}\cdot\mathbf{r}}\theta(k_{Fj}-k)\ . \tag{27}$$

We define

$$\tilde{I}^{(m)}_{jj'}(q)\equiv\tfrac{1}{2}\rho_j(0)\int d^3re^{i\mathbf{q}\cdot\mathbf{r}}I^{(m)}_{jj'}(r)S(k_{Fj}r) \tag{28}$$

and

$$\tilde{S}^{(j)}(q)\equiv 2\frac{\rho_j(0)}{2}\int d^3r\,e^{i\mathbf{q}\cdot\mathbf{r}}S(k_{Fj}r)\ , \tag{29}$$

where $\tilde{S}^{(j)}(q)$ is a 6×6 matrix. We look at elastic scattering in forward direction, so that $\mathbf{k}'=\mathbf{k}$. Substituting Eqs. (25) and (27)—(29) into Eq. (21) we arrive at

$$\tilde{U}^{(\mathrm{Pauli})}=-\left[\frac{1}{2\pi}\right]^3\sum_m\int_0^\infty q^2dq\int d\Omega_{k0}\,|\,Y_{1m}(\hat{\mathbf{k}}_0)\,|^2\tilde{S}(\mathbf{k}_0-\mathbf{q})\tilde{F}[\tilde{I}^{(m)}(\mathbf{q})-\tilde{I}^{(m)}(\mathbf{q})\tilde{I}^{(m)}(\mathbf{q})+\cdots]\ . \tag{30}$$

There is an overall factor of 2 in Eq. (30) arising from the sum over spin. This is explicit in the definition of $\tilde{S}$ in Eq. (29), which has an extra factor of 2 compared to Eqs. (27) and (28). The alternating sign is due to the rule that each hole line gets an additional minus sign. The overall sign arises because each term has one closed loop.

In Eq. (30), an infinite number of terms is included. We can sum up all these terms to give

$$\tilde{U}^{(\mathrm{Pauli})}=-\left[\frac{1}{2\pi}\right]^3\sum_m\int_0^\infty q^2dq\int d\Omega_{k_0}\,|\,Y_{1m}(\hat{\mathbf{k}}_0)\,|^2\tilde{S}(\mathbf{k}_0-\mathbf{q})\left[\frac{\tilde{F}\tilde{I}^{(m)}(\mathbf{q})}{1+\tilde{I}^{(m)}(\mathbf{q})}\right]\ . \tag{31}$$

We may integrate over the direction $\hat{\mathbf{k}}_0$ (instead of $\hat{\mathbf{q}}$) in Eqs. (30) and (31) because $\tilde{U}^{(\mathrm{Pauli})}$ is a rotationally invariant function of $\mathbf{k}_0$ and $\mathbf{q}$. It is convenient to do this and place $\hat{\mathbf{q}}$ along the z axis because $\tilde{I}$ [see Eq. (28)] is then diagonal in the magnetic quantum number. It is permissible to set $m'=m$ in Eq. (18) because of this choice of coordinate system.

Now we evaluate $\tilde{S}$ and $\tilde{I}$. From the definition of $\tilde{S}$ and the expression $\tilde{I}$ one finds

$$\tilde{S}^{(i)}(\mathbf{k}_0-\mathbf{q})=\begin{cases}2, & \text{if } |\mathbf{k}_0-\mathbf{q}| \le k_{Fi} \\ 0, & \text{if } |\mathbf{k}_0-\mathbf{q}| > k_{Fi}\end{cases} \tag{32}$$

and

$$\tilde{I}^{(m)}_{jj'}(q)=\tilde{F}_{jj'}h^{(m)}_j(q,k_{Fj}) , \tag{33}$$

where

$$h^{(0)}_j(q,k_{Fj})=\left[\frac{1}{2\pi}\right]^3\int_{q-k_{Fj}}^{q+k_{Fj}}p^2dp\frac{v^2(p)}{v^2(k_0)}\frac{1}{k_0^2-p^2+W+i\eta}\left[1-\left[\frac{p^2+q^2-k_{Fj}^2}{2pq}\right]^3\right], \tag{34}$$

$$h^{(1)}_j(q,k_{Fj})=h^{(-1)}_j(q,k_{Fj})=\left[\frac{1}{2\pi}\right]^3\int_{q-k_{Fj}}^{q+k_{Fj}}p^2dp\frac{v^2(p)}{v^2(k_0)}\frac{1}{k_0^2-p^2+W+i\eta}\left[1-\frac{3}{2}\left[\frac{p^2+q^2-k_{Fj}^2}{2pq}\right]+\frac{1}{2}\left[\frac{p^2+q^2-k_{Fj}^2}{2pq}\right]^3\right]. \tag{35}$$

Substituting Eqs. (32)—(35) into Eq. (31) we have

$$U^{(\text{Pauli})}_{jj}=-\left[\frac{1}{2\pi}\right]^3\sum_{j''}\tilde{F}_{jj''}\int_{k_0-k_{Fj}}^{k_0+k_{Fj}}dq\,q^2\sum_{m=0\pm1}A_m(q,k_{Fj})\left[\frac{\tilde{I}^{(m)}(q)}{1+\tilde{I}^{(m)}(q)}\right]_{j'',j} , \tag{36}$$

where

$$A_0=1-\left[\frac{k_0^2+q^2-k_{Fj}^2}{2k_0q}\right]^3 , \tag{37}$$

$$A_1=A_{-1}=1-\frac{3}{2}\left[\frac{k_0^2+q^2-k_{Fj}^2}{2k_0q}\right]+\frac{1}{2}\left[\frac{k_0^2+q^2-k_{Fj}^2}{2k_0q}\right]^3 . \tag{38}$$

V. SURFACE CORRECTION FOR FINITE NUCLEI

For finite nuclei there exists a nuclear surface which makes pion propagation different from what it is in the case of infinite nuclear matter. The nuclear matter result of the previous section is the first approximation in a systematic expansion[16] of the nuclear density matrix. We must accordingly interpret ρ_j as the density at **R**, the midpoint between the two nucleons struck in succession, and r in the argument of the Slater function as the magnitude of the distance between the struck nucleons. Corrections to the local density approximation of the density matrices are important in the surface. In Ref. 14, a correction was applied that was motivated by semiclassical scattering theory. According to this, the pion travels along trajectories parallel to the z axis, so that **R** is large and nearly perpendicular to **r**. It was argued that along such trajectories the density matrix should have an additional r dependence arising from the exponential falloff of the nuclear wave functions at large r. We adopt a similar approximation here and make the replacement

$$\rho_j S(k_{Fj}r)\to\rho_j(R)S_F(k_{Fj}r)e^{-r^2/8Ra} , \tag{39}$$

where a is the diffuseness of the density

$$a(R)=-\rho(R)/\rho'(R) \tag{40}$$

to take account of the nuclear surface. In this case we can write

$$\tilde{S}^{(i)}(\mathbf{k}_0-\mathbf{q})=\sum_l\tilde{S}^{(i)}_l(q)Y_{l0}(\hat{\mathbf{k}}_0) \tag{41}$$

and we find

$$\tilde{S}^{(i)}_l(q)=\rho_i(R)(4\pi)^{3/2}i^l(2l+1)\int_0^\infty r^2dr\,j_l(k_0r)j_l(qr)S(k_{Fi}r)e^{-r^2/8Ra} . \tag{42}$$

Similarly, we can write

$$\tilde{I}^{(m)}_{jj'}(q)=\tilde{F}_{jj'}J_j(k_0,q,m) \tag{43}$$

and one finds

$$J_j(k_0,q,m)=\tfrac{1}{2}\rho_j(R)\int\frac{d^3k_1}{(2\pi)^3}\frac{v^2(k_1)}{v^2(k_0)}Y^*_{1m}(\hat{\mathbf{k}}_1)Y_{1m}(\hat{\mathbf{k}}_1)\frac{1}{k_0^2-k_1^2+W+i\eta}\int d^3r\,e^{i(\mathbf{q}-\mathbf{k}_1)\cdot\mathbf{r}}S(k_{Fj}r)e^{-r^2/8Ra} . \tag{44}$$

If q is taken to be the z direction in the evaluation of the integration over r, one can find

$$J_j(k_0,q,m)=\rho_j(R)(-1)^m\frac{3}{8\pi}\sum_L C^{L0}_{1010}C^{L0}_{1m1-m}(ik_0)\int_0^\infty r^2dr\,j_L(qr)S(k_{Fj}r)e^{-r^2/8Ra}H_L(k_0,r,W) , \tag{45}$$

where

$$H_L(k_0,r,W)=\frac{2i}{\pi k_0}\int_0^\infty \frac{k_1^2 dk_1 j_L(k_1 r)}{k_0^2-k_1^2+W+i\eta}\frac{v^2(k_1)}{v^2(k_0)} \tag{46}$$

and $C^{LM}_{1m\,1m'}$ is the Clebsch-Gordan coefficient. By carrying out straightforward algebra we finally have

$$\tilde{U}^{(\text{Pauli})}=-\left[\frac{1}{2\pi}\right]^3\frac{3}{\sqrt{4\pi}}\sum_{l=0,2}\left[\frac{1}{2l+1}\right]^{1/2}C^{l0}_{1010}\int_0^\infty q^2 dq\,\tilde{S}_l(q)\sum_m(-1)^m C^{l0}_{1m\,1-m}\left[\frac{\tilde{F}\tilde{I}^{(m)}(q)}{1+\tilde{I}^{(m)}(q)}\right], \tag{47}$$

where $\tilde{U}$, $\tilde{F}$, and $\tilde{I}$ are 6×6 matrices.

If only the lowest order diagram is considered, the above equation can be greatly simplified. The result is

$$\tilde{U}^{(\text{lowest})}_{jj}=\frac{-3}{4\pi}\sum_{j'}\tilde{F}_{jj'}J^{(0)}_{jj'}\tilde{F}_{j'j} \tag{48}$$

and one can prove that

$$J^{(0)}_{jj'}=\frac{3k_0}{4\pi i}\sum_{l=0,2}|C^{l0}_{1010}|^2\rho_j(R)\rho_{j'}(R)\int_0^\infty r^2 dr\,\Gamma(r)j_l(k_0 r)S(k_{Fj}r)S(k_{Fj'}r)e^{-r^2/4Ra}H_L(k_0,r,W)\,. \tag{49}$$

From Eqs. (42)—(47) and Eqs. (22)—(24) we obtain the isoscalar, isovector, and isotensor parts of the pion-nucleus optical potential corresponding to the Pauli exchange terms.

VI. EIKONAL APPROXIMATION FOR THE PROPAGATOR

At medium energy the incident momentum of the projectile is quite large and the elementary cross section is often forward peaked. Therefore, the eikonal approximation is often used for the study of the pion nucleus interaction and reasonable results are obtained. In this section we investigate the effects due to the eikonal approximation for the propagator in the derivation of the optical potential. It is assumed that because nearly all scattering processes lead to small momentum transfer, the momentum of the incident particle in its passage through the nucleus is never likely to be very different from its incident momentum $\mathbf{k}_0$. To proceed with our discussion we assume that the form factor for pion-nucleon coupling is $v(k)=k$, which means that we do not cut off high momentum. In this case,

$$I^{(m)}_{jj'}(r)\Longrightarrow\tilde{F}_{jj'}\int\frac{d^3k_1}{(2\pi)^3}\frac{k_1^2}{k_0^2}|Y_{1m}(\hat{\mathbf{k}}_1)|^2\frac{e^{-i\mathbf{k}_1\cdot\mathbf{r}}}{k_0^2-k_1^2+W+i\eta}\,. \tag{50}$$

The straight line propagation implies that $\mathbf{k}_0\|\mathbf{k}_1$, so we can write

$$I^{(m)}_{jj'}(r)=\tilde{F}_{jj'}\frac{3}{4\pi}\frac{1}{k_0^2}G(r)\,, \tag{51}$$

where

$$G(r)=\left[\frac{1}{2\pi}\right]^3\int\frac{d^3k k^2 e^{-i\mathbf{k}\cdot\mathbf{r}}}{k_0^2-k^2+W+i\eta} \tag{52}$$

and W is a complex number for a given R and a given incident energy. We define $k_0'^2=k_0^2+W$, so that

$$G(r)=\left[\frac{1}{2\pi}\right]^3\int\frac{d^3k k^2 e^{-i\mathbf{k}\cdot\mathbf{r}}}{k_0'^2-k^2+i\eta}\,. \tag{53}$$

$G(r)$ can be reduced to

$$G(\mathbf{r})=-\delta(\mathbf{r})+k_0'^2\left[\frac{1}{2\pi}\right]^3\int\frac{d^3k e^{-i\mathbf{k}\cdot\mathbf{r}}}{k_0'^2-k^2+i\eta}\,. \tag{54}$$

If $r\neq 0$, we have

$$G(r)\approx k_0'^2\left[\frac{1}{2\pi}\right]^3\int\frac{d^3k e^{-i\mathbf{k}\cdot\mathbf{r}}}{k_0'^2-k^2+i\eta}\,. \tag{55}$$

If we write the variable of integration $\mathbf{k}$ as $\mathbf{k}=\mathbf{k}_0'+\boldsymbol{\Delta}$ where $\mathbf{k}_0'$ is in the direction of the incident pion and neglect Δ^2 in the denominator of the integrand then we may approximate the propagator by the integral

$$G(r)\approx -k_0'^2\left[\frac{1}{2\pi}\right]^3 e^{-i\mathbf{k}_0'\cdot\mathbf{r}}\int\frac{d^3\Delta e^{i\boldsymbol{\Delta}\cdot\mathbf{r}}}{2\boldsymbol{\Delta}\cdot\mathbf{k}_0'-i\eta}\,. \tag{56}$$

If we let z be the component of r parallel to $\mathbf{k}_0'$, this integral may be written as

$$G(r)\approx k_0'^2\left[\frac{i}{2k_0'}\right]\delta^{(2)}(\mathbf{b})e^{ik_0'z}\theta(z)\,. \tag{57}$$

Substituting Eqs. (53)—(57) into Eq. (44) we have

$$J_j(k_0,q,m)=\delta(m,0)\left[\frac{3}{4\pi}\right]\frac{\rho_i(R)}{4}(ik_0'/k_0^2)\times\int_0^\infty dz\,\Gamma(z)S(k_{Fj}z)e^{-z^2/8Ra}e^{i(q_{||}+k_0')z}\,. \tag{58}$$

From Eqs. (47)—(58), we can calculate the pion-nucleus optical potential in the eikonal approximation.

VII. CONNECTION TO OTHER THEORIES

Suppose we examine a simple model in which there is one species of massive nucleons filling a Fermi sea in an infinite medium. We represent the pion-nucleon interaction by a separable potential in p waves,

$$\langle \mathbf{k}' \mid V \mid \mathbf{k} \rangle = \lambda v(k')v(k) \sum_m Y^*_{1m}(\hat{\mathbf{k}}')Y_{1m}(\hat{\mathbf{k}}) \ . \tag{59}$$

The scattering T matrix satisfies the Lippmann-Schwinger equation

$$\langle \mathbf{k}' \mid T \mid \mathbf{k} \rangle = \langle \mathbf{k}' \mid V \mid \mathbf{k} \rangle + \int \frac{d^3k''}{(2\pi)^3} \langle \mathbf{k}' \mid V \mid \mathbf{k}'' \rangle \times \frac{1}{\omega_0 - \omega''_k + i\eta} \langle \mathbf{k}'' \mid T \mid \mathbf{k} \rangle \ , \tag{60}$$

where $\omega_k = (k^2+\mu^2)^{1/2}$. The solution of this equation is easily found and may be written

$$\langle \mathbf{k}' \mid T \mid \mathbf{k} \rangle = \tilde{\lambda} v(k')v(k) \sum_m Y^*_{1m}(\hat{\mathbf{k}}')Y_{1m}(\hat{\mathbf{k}}) \ , \tag{61}$$

where $\tilde{\lambda}$ is a function of energy and may be expressed in terms of λ and v.

For pion scattering in the medium, it is common[3-5,12,13] to introduce a "G matrix" for meson-nucleon scattering. One introduces the Pauli operator Q to exclude nucleon states below the Fermi surface. We may accordingly define the pion-nucleon G matrix T_g as

$$\langle \mathbf{k}' \mid T_g \mid \mathbf{k} \rangle = \langle \mathbf{k}' \mid V \mid \mathbf{k} \rangle + \int \frac{d^3k''}{(2\pi)^3} \langle \mathbf{k}' \mid V \mid \mathbf{k}'' \rangle \times \frac{Q(\mathbf{k}'',\mathbf{P})}{\omega_0 - \omega''_k + i\eta} \langle \mathbf{k}'' \mid T_g \mid \mathbf{k} \rangle \tag{62}$$

where

$$Q(\mathbf{k}'',\mathbf{P}) = \theta(\mid \mathbf{P} - \mathbf{k}'' \mid - p_F) \ . \tag{63}$$

The vector $\mathbf{P}$ is the total momentum of the pion and nucleon, and the θ function restricts the intermediate nucleon momentum $\mathbf{P}-\mathbf{k}''$ to be above the Fermi surface p_F. We may write the solution of Eq. (62) as

$$\langle \mathbf{k}' \mid T_g \mid \mathbf{k} \rangle = v(k')v(k) \sum_m Y^*_{1m}(\hat{\mathbf{k}}')\tilde{\lambda}^{(m)} Y_{1m}(\hat{\mathbf{k}}) \ . \tag{64}$$

A solution of this form holds only in a coordinate system for which $\mathbf{P}$ lies along the z axis; otherwise there are off-diagonal terms in magnetic quantum number.

It is convenient to express $\langle \mathbf{k}' \mid T_g \mid \mathbf{k} \rangle$ in terms of $\langle \mathbf{k}' \mid T \mid \mathbf{k} \rangle$. This is given as

$$\langle \mathbf{k}' \mid T_g \mid \mathbf{k} \rangle = \langle \mathbf{k}' \mid T \mid \mathbf{k} \rangle + \int \frac{d^2k''}{(2\pi)^3} \langle \mathbf{k}' \mid T \mid \mathbf{k}'' \rangle \times \frac{Q(\mathbf{k}'',\mathbf{P}) - 1}{\omega_0 - \omega''_k + i\eta} \langle \mathbf{k}'' \mid T_g \mid \mathbf{k} \rangle \ . \tag{65}$$

Substituting Eqs. (61) and (64) into (65) we find

$$\tilde{\lambda}^{(m)}(\mathbf{P}) = \frac{\tilde{\lambda}}{1+\tilde{I}^{(m)}_g(\mathbf{P})} \ , \tag{66}$$

where

$$\tilde{I}^{(m)}_g(\mathbf{P}) = \tilde{I}^{(m)}_g(-\mathbf{P}) \equiv v^2(k_0)\tilde{\lambda} \int \frac{d^3k''}{(2\pi)^3} \frac{v^2(k'')}{v^2(k_0)} \frac{\mid Y_{1m}(\hat{\mathbf{k}}'') \mid^2}{\omega_0 - \omega''_k + i\eta} \times \theta(p_F - \mid \mathbf{P} - \mathbf{k}'' \mid) \mid_{\mathbf{P} \mid\mid \hat{z}} \ . \tag{67}$$

Note that $\tilde{I}^{(m)}(\mathbf{P})$ depends only on $\mid \mathbf{P} \mid$ because of our choice of z axis. Thus we have

$$\langle \mathbf{k}' \mid T_g \mid \mathbf{k} \rangle = v(k')v(k)\tilde{\lambda} \sum_m \frac{Y^*_{1m}(\hat{\mathbf{k}}')Y_{1m}(\hat{\mathbf{k}})}{1+\tilde{I}^{(m)}_g(\mathbf{P})} \ . \tag{68}$$

To get the U^{Pauli} plus the lowest order optical potential $U^{(0)}$ in terms of T_g we must sum over the nucleon states (including two spin directions)

$$\sum_A \rightarrow 2 \int_{p<p_F} \frac{d^3P}{(2\pi)^3} \ . \tag{69}$$

Then,

$$U^{(0)} + U^{\text{Pauli}} = 2 \int_{p<p_F} \frac{d^3P}{(2\pi)^3} \langle \mathbf{k}' \mid T_g \mid \mathbf{k} \rangle \ . \tag{70}$$

However, because we have chosen the direction of $\hat{\mathbf{P}}$ as the z axis, we cannot immediately integrate over $\mathbf{P}$. From the fact that $\langle \mathbf{k}' \mid T_g \mid \mathbf{k} \rangle$ is a scalar function of three vectors, $\mathbf{k}'$, $\mathbf{k}$, and $\mathbf{P}$, we know that its value is independent of the choice of z axis and it is a simple matter to place the z axis along $\hat{\mathbf{k}}'$ or $\hat{\mathbf{k}}$ using the rotation matrices[17] $D^m_{m'J}(\alpha,\beta,\gamma)$. In nuclear matter we want the case $\hat{\mathbf{k}}' = \hat{\mathbf{k}}$ and the result is

$$\langle \mathbf{k} \mid T_g \mid \mathbf{k} \rangle = v^2(k_0)\tilde{\lambda} \sum_m \frac{\mid Y_{1m}(\hat{\mathbf{P}}) \mid^2}{1+\tilde{I}^{(m)}(P)} \tag{71}$$

so

$$U^{(0)} + U^{\text{Pauli}} = 2\tilde{F} \sum_m \int \frac{P^2 dP}{(2\pi)^3} \frac{1}{1+\tilde{I}^{(m)}(P)} \times \int d\hat{\mathbf{P}} \mid Y_{1m}(\hat{\mathbf{P}}) \mid^2 \theta(P_F - \mid \mathbf{P} - \mathbf{k} \mid) \ . \tag{72}$$

To make a connection with the results of Sec. IV, note that $\tilde{I}_g(\mathbf{P})$ is the same as $\tilde{I}$ in Eqs. (18) and (28) if we set the pair distribution function $\Gamma = 1$, $W = 0$, use the pion propagator $(\omega_0 - \omega_k + i\eta)^{-1}$ instead of $(k_0^2 - k^2 + i\eta)^{-1}$, and make use of the connection $f = -4\pi T$ between the T matrix and scattering amplitude.

We have thus shown that our definition of the set of diagrams in Eq. (2) gives back the normal Pauli G matrix of Eq. (62) under the set of approximations given above, which makes the connection to Refs. 3–5, 12, and 13. We hasten to point out that the G-matrix treatment of the Pauli effect was strongly criticized in Ref. 6 because the nonstatic corrections arising from the negative frequency components of the pion propagator are not incorporated. Because our treatment in Secs. II–V (and the numerical results we present in Sec. VII) is built upon the field theoretical meson propagator and not the linear propaga-

TABLE I. Optical potential for ^{18}O corresponding to Pauli exchange terms of Fig. 2. U_0, U_1, and U_2 are the isoscalar, isovector, and isotensor potentials, respectively, calculated for $\beta=4.87$ fm^{-1}, $\rho(R)=\rho(3.5\text{ fm})$, and $\Delta\rho/\rho=(N-Z)/A=0.111$.

T_π (MeV)	U_0 (fm^{-2})	U_1 (fm^{-2})	U_2 (fm^{-2})
50	$(-0.32-0.44i)\times10^{-2}$	$(-0.56-0.89i)\times10^{-3}$	$(-0.04\ -0.80i)\times10^{-4}$
100	$(0.79-2.24i)\times10^{-2}$	$(1.97-4.02i)\times10^{-3}$	$(2.16\ -2.64i)\times10^{-4}$
150	$(4.80+0.67i)\times10^{-2}$	$(7.99+1.99i)\times10^{-3}$	$(4.16\ +2.21i)\times10^{-4}$
200	$(0.53+4.27i)\times10^{-2}$	$(0.53+7.01i)\times10^{-3}$	$(-0.036+3.55i)\times10^{-4}$
250	$(-1.81+1.97i)\times10^{-2}$	$(-3.10+3.17i)\times10^{-3}$	$(-1.69\ +1.63i)\times10^{-4}$
300	$(-1.56+0.45i)\times10^{-2}$	$(-2.70+0.64i)\times10^{-3}$	$(-1.59\ +0.23i)\times10^{-4}$

tor [see Eq. (60)], this criticism does not apply to the present treatment. We also prefer using the diagrammatic analysis because it allows us to extend the theory to finite nuclei in a straightforward fashion, and permits additional effects to be incorporated naturally, such as short-range nucleon-nucleon correlations (including the rho meson) and pion mean-free path corrections. All of these corrections, we believe, are essential to getting the physics correct and they are difficult to incorporate in other approaches.

VIII. NUMERICAL RESULTS FOR THE OPTICAL POTENTIAL

We show in this section numerical results appropriate to the finite nucleus ^{18}O. Because we find the integrals more stable in finite nuclei as a consequence of the surface correction and inclusion of the pion medium modifications, we have not made extensive calculations for infinite nuclear matter. In this paper our interest is mainly the resonance region. From previous work[18] we know that the important region of the nucleus for scattering at these energies is the surface near $R=\bar{R}$ where, for ^{18}O, $\bar{R}=3.5$ fm and $\rho(\bar{R})/\rho_0\simeq0.2$ ($\rho_0\equiv0.16$ fm^{-3} is approximately the density at the center of nuclei). We therefore show results only for relatively low densities, $\rho/\rho_0\lesssim0.5$. The value $\bar{R}$ used here is the same as that in Ref. 14 for the evaluation of the second-order optical potential. In all of our calculations, we have taken $v(k)$ to have the form

$$v(k)=k(1+k^2/\beta^2)^{-1} \tag{73}$$

with $\beta=4.82$ fm^{-1}. We have also used the phase-shift analysis of Ref. 19 to obtain the pion-nucleon parameters. For the nuclear density, we have taken a two-parameter Fermi shape with a half-density radius $R_c=1.1A^{1/3}$ fm, and diffuseness $a=0.56$ fm for both neutrons and protons. We calculate the various parts of the optical potential for incident pion kinetic energies ranging from 50 to 300 MeV. In Table I we summarize our numerical results for on-shell values of the optical potential evaluated in momentum space.

For practical applications it is useful to parametrize the optical potential as a function of ρ and $\Delta\rho$. One such parametrization was suggested in Ref. 14. For $\mathbf{k}=\mathbf{k}'=\mathbf{k}_0$, $T=1$, it assumes the following form:

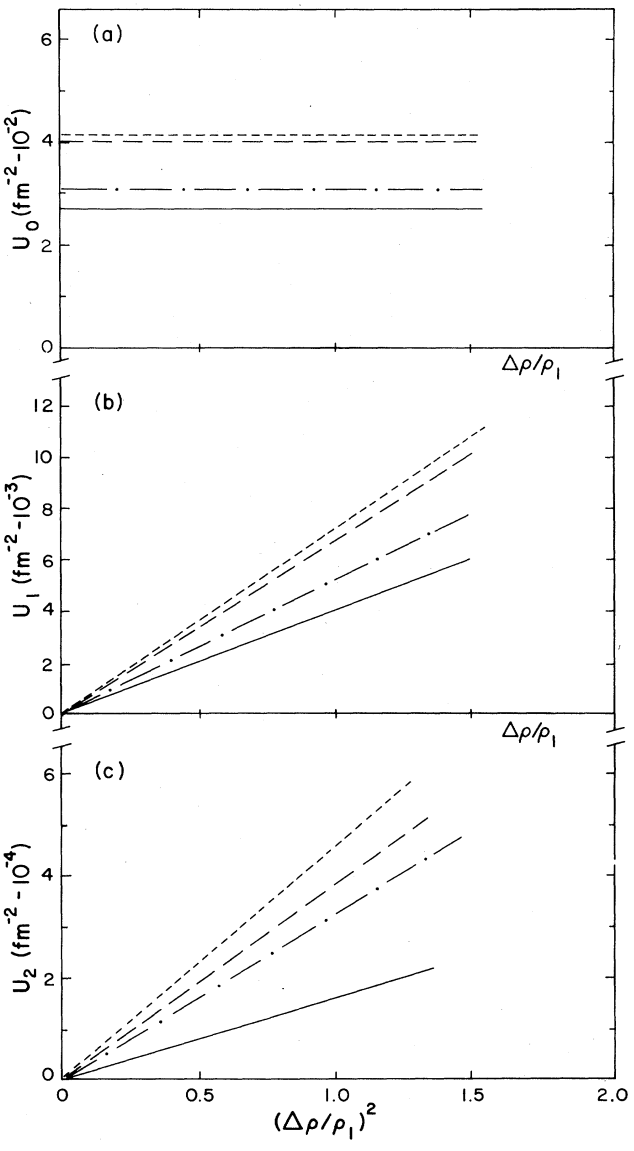

FIG. 3. Dependence of isoscalar (U_0), isovector (U_1), and isotensor potential (U_2) on the valence neutron density $\Delta\rho$. The unit of $\Delta\rho$ in $\rho_1=3.62\times10^{-3}$ fm^{-3}. The solid curve is the real part of the full calculation and the long dashes the imaginary part of the full calculation. The real and imaginary parts of the lowest order calculation are, respectively, the dot-dashed and short dashed curves.

$$U_0=-k_0^2\left[\frac{\rho^2}{\rho_0}\lambda_0+\frac{\Delta\rho^2}{\rho_0}\lambda_3-\frac{\Delta\rho^2}{\rho_0}\lambda_2\right], \tag{74}$$

$$U_0=-k_0^2\left[\frac{1}{2}\rho\frac{\Delta\rho}{\rho_0}\lambda_1+\frac{1}{2}\frac{\Delta\rho^2}{\rho_0}\lambda_2\right], \tag{75}$$

$$U_2=-k_0^2\frac{\Delta\rho^2}{\rho_0}\lambda_2 . \tag{76}$$

In Fig. 3 we show the dependence of the optical potential on $\Delta\rho(r)/\rho_1$ for fixed $\rho(r)/\rho_0=0.2$, which is the density at $R=3.5$ fm for ^{18}O, and at pion incident kinetic energy $T_\pi=180$ MeV. Here $\rho_0\equiv 0.16$ fm^{-3}, which is approximately the central density of nuclei. The unit ρ_1 of $\Delta\rho(r)$ is $\rho_1=3.62\times10^{-3}$ fm^{-3}, which is approximately[18] the valence neutron density at $\bar{R}$ in ^{18}O in Hartree-Fock calculations. It is interesting to notice that the isoscalar part of the optical potential does not depend on the valence neutron density for fixed total density of the nucleus. The isovector part of the potential can be approximately parametrized to be proportional to $\Delta\rho(r)/\rho_1$. The isotensor potential is plotted as a function of $\Delta\rho(r)^2/\rho_1^2$. We observe that the real and imaginary parts of the optical potential, to a good approximation, lie on straight lines. The same situation occurs for other pion energies and densities up to $\rho/\rho_0\simeq 0.5$. This calculation confirms the dependence of Eqs. (74)—(76) on $\Delta\rho$, even when higher order effects are included. The figure also shows the dependence of the lowest-order calculation on $\Delta\rho$.

The $\rho(r)$ dependence of the optical potential is obtained by taking a fixed $\Delta\rho(r)$ and changing $\rho(r)$. In this case, it is more complicated because the pion mean free path and the surface exponential falloff correction are functions of $\rho(r)$. We evaluate W and make the surface correction at fixed $R=3.5$ fm, and change $\rho(r)$ to calculate the optical potential. We found that the following dependences hold to a very good approximation:

$$U_0\propto\rho(r)^{5/3} , \tag{77}$$

$$U_1\propto\rho^{2/3} , \tag{78}$$

$$U_2\propto\rho^{2/3} . \tag{79}$$

Equations (77)—(79) have a different dependence on ρ than Eqs. (74)—(76). However, the density dependence of W and the surface correction may change this. We show the effect of this in Fig. 4 where we have plotted the den-

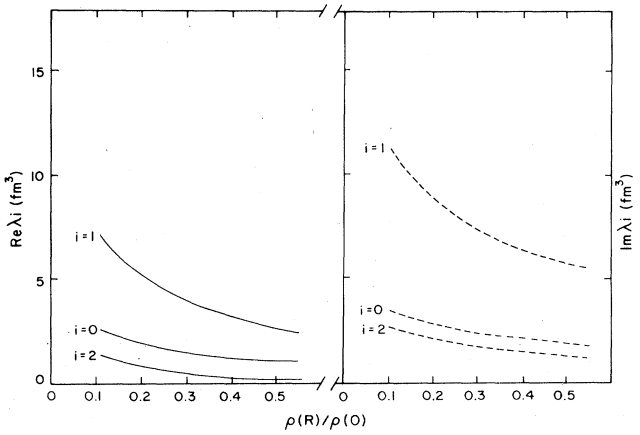

FIG. 4. Dependence of λ_i on ρ/ρ_0. The solid line is the real part of λ and the dashed line the imaginary part.

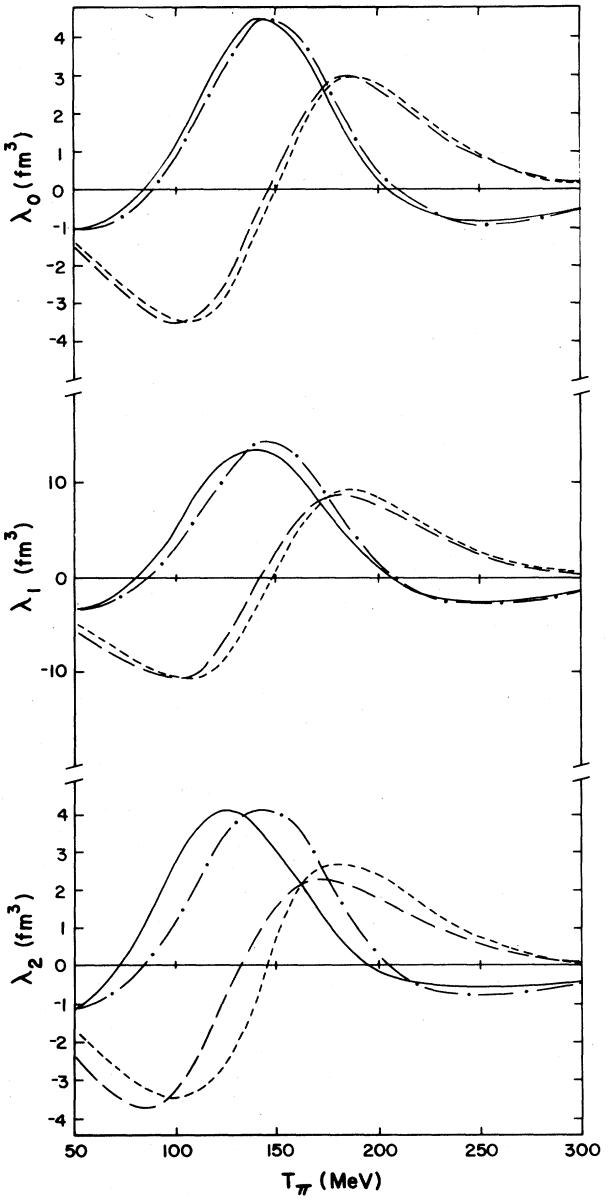

FIG. 5. Comparison of full calculation to lowest order results. The solid line is the real part of the full calculation and the long dashes the imaginary part of the full calculation. The real and imaginary parts of the lowest order calculation are, respectively, the dot-dashed and short-dashed curves.

TABLE II. Convergence of series in Fig. 2 as a function of density.

	Lowest order			Full calculation		
ρ/ρ_0	λ_0	λ_1	λ_2	λ_0	λ_1	λ_2
			180 MeV			
0.2	$2.25+2.95i$	$6.83+9.49i$	$1.88+2.65i$	$1.94+2.86i$	$5.16+8.85i$	$0.88+2.19i$
0.36	$1.76+2.30i$	$5.23+7.44i$	$1.50+2.25i$	$1.39+2.20i$	$3.45+6.72i$	$3.88+1.63i$
0.75	$0.43+1.85i$	$2.73+5.60i$	$0.75+1.84i$	$0.62+1.47i$	$1.31+4.44i$	$-0.047+0.89i$
			50 MeV			
0.75	$-0.97-1.12i$	$-3.03-4.10i$	$-1.00-1.79i$	$-1.03-1.43i$	$3.28-6.16i$	$1.03-4.26i$

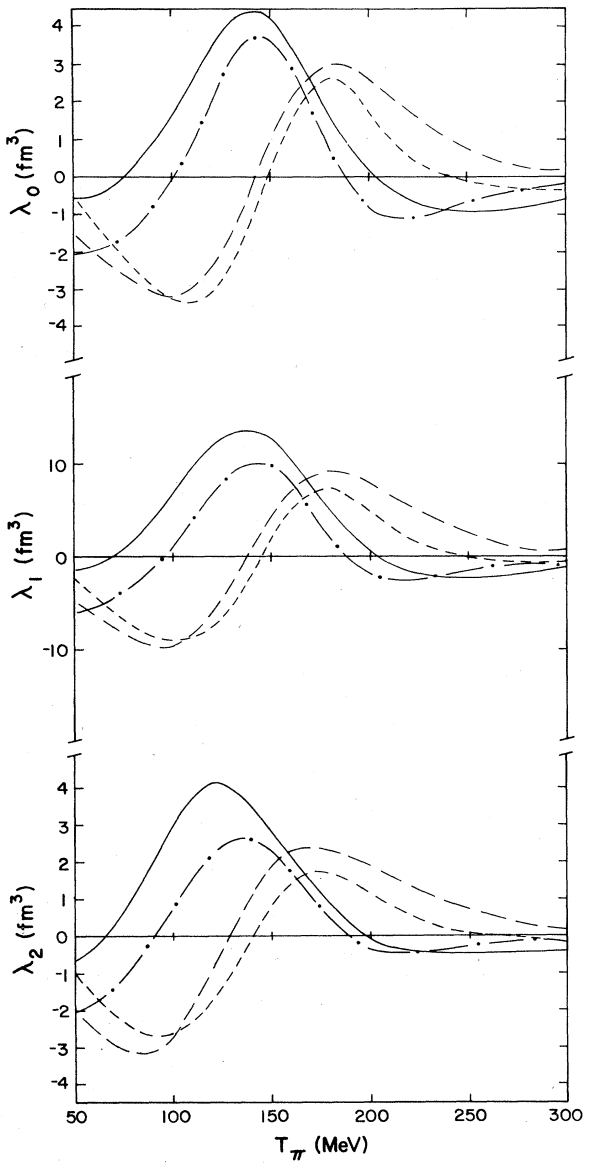

FIG. 6. Comparison of full calculation to eikonal approximation. The solid line shows the real part of the full calculation and the long dashes the imaginary part. The real and imaginary parts in the eikonal approximation are, respectively, the dot dashed and short-dashed curves.

sity dependence of λ_i [defined by Eqs. (74)—(76)]. The quantities λ_0, λ_1, and λ_2 now have a slightly stronger density dependence. The results are similar to those of Ref. 14. Clearly the precise form of the density dependence depends on the details of the calculation.

Now we investigate the convergence of the expansion. From Eq. (48) we can calculate the lowest order contribution. In the upper part of Table II we show the lowest order and full calculation at three densities for $T_\pi=180$ MeV. The rate of convergence is not much different up to $\rho/\rho_0=0.36$. At $\rho/\rho_0=0.75$ we eliminated the surface correction and the convergence is noticeably worse, especially for λ_2. In the lower part of Table II we show the results for 50 MeV at $\rho/\rho_0=0.75$. At low energies one expects that the higher densities will become more important. Convergence appears to be better than it is at 180 MeV, because the interaction is weaker. At low energy the Pauli corrections in both s- and p-waves should be considered, but here we have studied convergence for the p-wave piece only.

In Fig. 5 we compare our full calculation with the lowest order results for the pion incident energies between 50 and 300 MeV for $\rho/\rho_0=0.20$. We find the following: (1) The higher order terms give a rather large correction to the isotensor part of the potential for pion incident energies below 200 MeV. At some energies the potentials can differ by a factor of 2 and even have different phase. (2) The contributions to U_0 and U_1 from higher order terms are relatively small. This is especially true for the isoscalar part of the optical potential. (3) Above 200 MeV, the higher order correction is small, less than 30%. As a rule of thumb, the effects of higher order shift the lowest order downward by 4 MeV for the isoscalar, 7 MeV for the isovector, and 15 MeV for the isotensor interaction.

The lowest order calculations here give the same results as in Ref. 14 if the elementary amplitude is taken to be the same. But here we use a different method to compute the Pauli exchange terms.

We calculate the optical potential with the eikonal approximation, using Eq. (58) for different energies and compare with the results from Eq. (44). In Fig. 6 we give two different results. We see that the energy dependences of the various parts of the potentials with and without the eikonal approximation are not far from each other. Generally, the eikonal approximation makes the optical potential smaller. Around 160 MeV, the overall difference is

TABLE III. Dependence of λ_i on form factor cutoff β in Eq. (73).

T_π (MeV)	100		150		200		250		300	
β	4.82	48.2	4.82	48.2	4.82	48.2	4.82	48.2	4.82	48.2
λ_0 (fm^3)	1.23	1.59	4.37	4.23	0.33	0.14	−0.80	−0.81	−0.53	−0.52
	$-3.49i$	$-3.12i$	$+0.61i$	$+1.09i$	$+2.62i$	$+2.58i$	$+0.87i$	$+0.84i$	$+0.15i$	$+0.16i$
λ_1 (fm^3)	5.18	6.38	13.00	12.46	0.59	0.11	−2.46	−2.47	−1.63	−1.61
	$-10.88i$	$-9.90i$	$+3.20i$	$+4.46i$	$+7.55i$	$+7.54i$	$+2.51i$	$+2.43i$	$+0.38i$	$+0.40i$
λ^2 (fm^3)	2.69	2.88	3.07	2.82	−0.017	−0.07	−0.61	−0.61	−0.43	−0.43
	$-3.31i$	$-2.86i$	$+1.63i$	$+1.83i$	$+1.76i$	$+1.72i$	$+0.59i$	$+0.57i$	$+0.06i$	$+0.70i$

less than 30%. This comparison gives some measure of the importance of the real part of the pion propagator in calculating the exchange effects.

Within the eikonal approximation for the propagation of the pion, the Pauli exchange series converges faster. We found that in all cases the lowest order diagram accounts for most of the Pauli exchange contributions.

To give some idea of the dependence of our results on β in Eq. (73) see Table III. The results are insensitive to this parameter.

In Table IV we show the effect of dressing the pion propagator according to Fig. 2(c). W now includes the term in Eq. (20) and in addition the result $U^{(\mathrm{Pauli})}$. Those modifications do not lead to a significant modification of the results.

IX. SUMMARY AND CONCLUSIONS

We have evaluated Pauli effects in the optical potential formulation of Refs. 14 and 15. The theory is different from the familiar G-matrix formulation, in which the Pauli principle leads to a restriction on intermediate states that can occur in the pion-nucleon scattering amplitude. In our theory, nucleons are excluded from states below the Fermi surface by explicit evaluation of exchange terms. We presented an integral equation which sums to all orders a specific set of exchange terms and showed that a special case of the solution gives the π-nucleon G matrix for infinite nuclear matter. We have considered corrections to this, which arise from the nuclear surface and pion-nucleus interactions. We are also able to avoid imposing the time-ordering restrictions that occur in the G-matrix approach, namely that pions propagate only forward in time. Our theory has the additional advantage that it leads to an explicit procedure for using isospin invariance to evaluate the isovector and isotensor optical potentials required for studying pion charge exchange. One of our main interests was to study the convergence of the expansion that leads to $U^{(\mathrm{Pauli})}$.

In order to study the convergence we have made a few approximations. The main ones are to neglect the spin dependence of the pion-nucleon amplitude and to retain only the p-wave interaction. In the region of the Δ_{33} resonance, the corrections are not expected to be large. We have also used a local density approximation to the nuclear density matrix to include surface effects. We found that for the purposes of evaluating scattering in the resonance region, the convergence of the expansion is quite fast, and that the dominant effects in the isoscalar and isovector interaction arise already in the lowest order of our expansion (which is second order in the πN scattering amplitude). For the isotensor interaction, the qualitative behavior is obtained in lowest order. As an approximate rule for obtaining the complete result, we found that a shift of the lowest order result downward by 4 MeV for the isoscalar, 7 MeV for the isovector, and 15 MeV for

TABLE IV. Results of calculating λ_i with the Pauli effect on the mean-free path W in Eq. (20). Column 1 is without the Pauli correlations and column 2 includes them.

T_π (MeV)	100		150		200		250		300	
Iteration	1	2	1	2	1	2	1	2	1	2
λ_0 (fm^3)	1.23	1.26	4.38	4.37	0.33	0.29	−0.80	−0.79	−0.53	−0.52
	$-3.49i$	$-3.58i$	$+0.61i$	$+0.75i$	$+2.62+$	$+2.57i$	$+0.87i$	$+10.87i$	$+0.15i$	$+0.16i$
λ_1 (fm^3)	5.18	5.36	12.8	12.7	0.59	0.50	−2.42	−2.38	−1.60	−1.59
	$-10.88i$	$-11.16i$	$+3.08i$	$+3.50i$	$+7.55i$	$+7.41i$	$+2.47i$	$+2.46i$	$+0.38i$	$+0.39i$
λ_2 (fm^3)	2.69	2.80	3.07	2.99	−0.018	−0.029	−0.61	−0.60	−0.43	−0.43
	$-3.31i$	$-3.39i$	$+1.63i$	$+1.72i$	$+1.78i$	$+1.72i$	$+0.59i$	$+0.58i$	$+0.064i$	$+0.066i$

the isotensor interaction will give the full result.

We also examined the use of the eikonal approximation to the pion propagator in evaluating Pauli effects. We found that the eikonal approximation leads to similar results but tends to underestimate the exchange effects.

Our conclusion is that Pauli exchange terms are easily incorporated perturbatively. This result provides additional encouragement for using a microscopic optical model approach as a means of evaluating pion-nucleus scattering.

One of the authors (H.C.C.) is grateful to all friends at LAMPF for the very kind hospitality and help extended to him during his stay in Los Alamos.

---

*Permanent address: Institute of High Energy Physics, Academia Sinica, Beijing, People's Republic of China.

[1]S. J. Greene, C. Harvey, P. A. Seidl, R. Gilman, E. R. Siciliano, and M. B. Johnson, Phys. Rev. C **30**, 2003 (1984).

[2]C. B. Dover, J. Hufner, and R. H. Lemmer, Ann. Phys. (N.Y.) **66**, 24B (1971); C. B. Dover and R. H. Lemmer, Phys. Rev. C **7**, 2312 (1973).

[3]H. A. Bethe, Phys. Rev. Lett. **30**, 105 (1973).

[4]J. M. Eisenberg and H. J. Weber, Phys. Lett. **45B**, 110 (1973); H. J. Weber and J. M. Eisenberg, Phys. Rev. C **10**, 925 (1974).

[5]R. H. Landau and M. McMillan, Phys. Rev. C **8**, 2094 (1973); R. H. Landau and A. W. Thomas, Nucl. Phys. **A302**, 461 (1978).

[6]C. B. Dover and R. H. Lemmer, Phys. Rev. C **14**, 2211 (1976).

[7]M. Hirata, F. Lenz, and K. Yazaki, Ann. Phys. (N.Y.) **108**, 116 (1977).

[8]A. Reitan, Nucl. Phys. **B68**, 387 (1974).

[9]E. Oset, D. Strottman, and G. E. Brown, Phys. Lett. **73B**, 393 (1978); E. Oset, Phys. Lett. **65B**, 46 (1976).

[10]X. Liu, Z. Wu, Z. Huang, and Y. Li, Sci. Sin. **24**, 789 (1981).

[11]K. P. Lohs and A. Gal, Nucl. Phys. **A292**, 375 (1977).

[12]J. de Kam, F. Van Geffem, and M. Van der Velde, Nucl. Phys. **A333**, 443 (1980); J. de Kam, Phys. Rev. C **24**, 1554 (1981).

[13]W. B. Kaufmann and W. R. Gibbs, Phys. Rev. C **28**, 1286 (1983).

[14]M. B. Johnson and E. R. Siciliano, Phys. Rev. C **27**, 730 (1983).

[15](a) M. B. Johnson and D. J. Ernst, Phys. Rev. C **27**, 709 (1983); (b) M. B. Johnson and D. J. Ernst (unpublished).

[16]J. W. Negele and D. Vantherin, Phys. Rev. C **5**, 1472 (1972); **11**, 1031 (1975).

[17]D. M. Brink and G. R. Satchler, *Angular Momentum* (Clarendon, Oxford, 1968).

[18]M. B. Johnson, Phys. Rev. C **22**, 192 (1980).

[19]G. Rowe, M. Salomon, and R. H. Landau, Phys. Rev. C **18**, 584 (1978).